

Dynamics of a coplanar-electrode plasma display panel. II. Cell optimization

Shahid Rauf^{a)} and Mark J. Kushner^{b)}

*Department of Electrical and Computer Engineering, University of Illinois, 1406 West Green Street
Urbana, Illinois 61801*

(Received 17 September 1998; accepted for publication 7 January 1999)

Plasma display panels (PDPs) are a leading technology for large-area flat panel displays. As a result, there is significant interest in improving their efficiency, luminosity, and lifetime. In this article, results from a two-dimensional model are used to investigate the consequences of operating conditions, gas mixture, cell dimensions, and material properties on the visible light generation capacity (luminosity and efficiency) of a coplanar-electrode PDP cell sustained in He/Ne/Xe gas mixtures. Of the species that dominantly lead to the generation of visible light (Xe^* , Xe^{**} , and Xe_2^*), Xe_2^* makes the largest contribution for our conditions since its UV radiation is optically thin and Xe_2^* is efficiently generated from the long-lived xenon metastable. Significant improvements could be made in PDP light generation efficiency by choosing operating conditions that favor production of Xe_2^* , such as increasing gas pressure to enhance the three-body collision processes that generate Xe_2^* . Gas mixtures with more Ne (or less He) were found to produce more visible light at higher efficiency since electron transport in Ne is less collisional than He and Xe_2^* is produced more efficiently in three body collisions with Ne. PDP light emission characteristics are sensitive to the spacing between the dielectrics and there is an optimum spacing where both total visible light output and efficiency are high. It was found that PDP cells do not generate visible light efficiently during the postavalanche discharge phase due to low values of E/N (electric field/total gas density) in the bulk plasma region. Slight improvements can be made in light generation efficiency by choosing conditions for which PDP cell spends less time in the discharge phase in each cycle. © 1999 American Institute of Physics. [S0021-8979(99)07207-2]

I. INTRODUCTION

Plasma display panels (PDPs) are one of the leading technologies currently under development for large-area high-brightness flat panel displays.¹⁻³ As a result there is considerable interest in improving the luminance and efficiency of PDPs for mass-market television displays.¹ There are also concerns regarding PDP operating lifetime, which may require design improvements that minimize ion bombardment of phosphors. These improvements will most likely result from a careful optimization of the cell design, operating conditions, voltage pulse characteristics, and gas composition, an endeavor that can benefit from a detailed understanding of the dynamics of PDP cells. To investigate these issues, we developed a two-dimensional hybrid simulation for the direct-current (dc) pulsed plasma operation of PDP cells, and applied the model to a coplanar-electrode PDP cell sustained in He/Ne/Xe gas mixtures, a schematic of which is shown in Fig. 1(a) of the companion paper (Paper I).⁴ In Paper I, we used the results from the model to describe the electrostatics of the PDP cell and processes that lead to visible light generation. Using these basic operating principles as a guide, we investigated the effect of operating conditions, gas composition, and cell design on the light gen-

eration capacity and efficiency of PDP cells, and these results are discussed in this article. Previous theoretical investigations on the operation of PDP cells and their relationship to the present work are summarized in Paper I.

In Sec. II, we briefly describe the PDP model. The results of parametric studies are discussed in Sec. III, and key observations are summarized in Sec. IV.

II. DESCRIPTION OF THE PDP MODEL

The PDP model used in this investigation is described in detail in Paper I. For the parametric studies described in this article, the local field approximation (LFA) was used to determine electron transport coefficients and rate coefficients for electron impact reactions. As explained in Paper I and Ref. 5, results using the LFA are reasonably accurate and should correctly predict the major trends.

In this article, we will compare total energy deposition (E), visible light fluence (L), and light generation efficiency (η) of the PDP cell for different operating conditions. These quantities are defined over the time interval (t_1, t_2) as

$$E = \int_{t_1}^{t_2} dt \int_V dx dy \mathbf{j} \cdot \mathbf{E}$$

$$= \int_{t_1}^{t_2} dt \int_V dx dy \nabla \phi \cdot \sum_{i=1}^{N_{\text{ch}}} [q_i (D_i \nabla n_i + (q_i / |q_i|) \mu_i n_i \nabla \phi)],$$
(1)

$$L = \int_{t_1}^{t_2} \Phi dt,$$
(2)

^{a)}Present address: Motorola, Embedded Systems Technology Laboratory, 3501 Bluestein Blvd., Austin, TX 78721.

Electronic mail: ra8952@email.sps.mot.com

^{b)}Author to whom correspondence should be addressed. Electronic mail: mjk@uiuc.edu

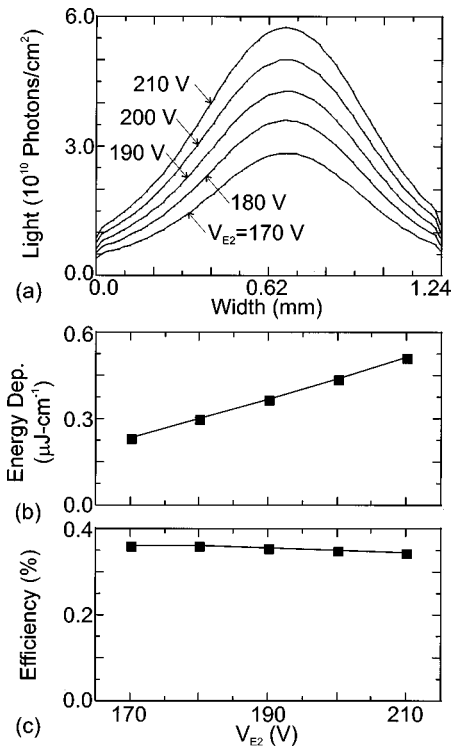


FIG. 1. Effect of varying the applied voltage amplitude on E_2 during the second pulse ($4\text{--}10\ \mu\text{s}$) on (a) visible light fluence, (b) total energy deposition, and (c) light generation efficiency.

$$\eta = W_{\text{ph}} \int_{\text{Window}} L dx / E, \quad (3)$$

where ϕ , Φ , W_{ph} , and N_{ch} are the electrical potential, visible photon flux, energy of visible light photons, and number of charged species. n_i , q_i , D_i , and μ_i are, respectively, the number density, charge, diffusion coefficient, and mobility of species i . In the results described here, $t_1 = 4.0\ \mu\text{s}$ and $t_2 = 10.0\ \mu\text{s}$, which corresponds to the second in a series of voltage pulses [Fig. 1(b) of Paper I]. To compute light generation efficiency, we assumed that $W_{\text{ph}} = 2.5\ \text{eV}$, which corresponds to a wavelength of $4960\ \text{\AA}$.

III. OPTIMIZATION OF THE PDP CELL

The efficiency and luminosity of PDP cells sensitively depend on the input voltage pulse shape, gas composition, gas pressure, cell dimensions, placement of electrodes, and material properties. In this section, we use results from the PDP model to describe the consequences of varying these factors on PDP performance for a coplanar-electrode cell⁶ operating with He/Ne/Xe gas mixtures. The cell design is shown in Fig. 1(a) of Paper I, and the input voltage wave forms are shown in Fig. 1(b) of Paper I.

The operation of the device has been described in detail in Paper I for conditions that will be referred to as the base case. The gas mixture for the base case is He/Ne/Xe = 70/26/4, at 400 Torr gap length $d = 150\ \mu\text{m}$, electrode length $l = 300\ \mu\text{m}$, electrode separation $l_e = 100\ \mu\text{m}$, dielectric thickness below the electrodes $d_d = 25\ \mu\text{m}$, and dielectric constant of the upper dielectric $\epsilon/\epsilon_0 = 15$. 200 V is ap-

plied to E_1 during the first pulse. The voltage is reduced to 180 V during the subsequent pulses for the base case. As discussed in Paper I, the first voltage pulse on E_1 usually initiates a discharge between the top biased electrode and the grounded lower address electrode. The surface of the lower dielectric is positively charged during this pulse. From the second pulse onward, this positive charge reduces the y -directed electric field and the discharge shifts to between the two top electrodes, E_1 and E_2 . In the following discussion we will use results from the second pulse ($4\text{--}10\ \mu\text{s}$) where a positive voltage is applied to E_2 and E_1 is grounded. Excited state densities are reduced to small values at $4\ \mu\text{s}$ so emission resulting from the first pulse does not effect the light emission characteristics of the second pulse.

We first investigate the consequence of varying the applied voltage amplitude V_0 on PDP performance. It is well known that increasing V_0 increases visible light emissions, although this is often not the most viable option due to limits on power dissipation and an increase in the energy or fluence of ions incident on the dielectric surfaces which reduces the device lifetime. The results for varying applied voltage can, however, be used as a benchmark against which other methods of improving efficiency can be compared. The total visible light emission from the top of the cell during the voltage pulse ($4\text{--}10\ \mu\text{s}$), total energy deposited in the gas, and the light generation efficiency are shown in Fig. 1 as a function of the applied voltage on E_2 . (Energy deposition is expressed per unit length in the dimension not resolved in the simulation.)

Once the plasma has been initiated, the discharge remains active as long as the voltage across the gap is above a critical value. Flow of current which charges the dielectric's capacitance reduces the gap voltage and eventually quenches the discharge. In this regard, the PDP cell operation is analogous to a dielectric barrier discharge (DBD)⁷ and scales in a similar manner. When the applied voltage amplitude is increased, while the breakdown voltage and self-sustaining voltages do not change, more current is required to charge the dielectric surfaces before the gap voltage is reduced below the minimum for discharge sustenance. Since the device remains in the discharge phase (with a large electron density) for a longer period of time, more electron impact excitation collisions occur resulting in more visible light output [Fig. 1(a)]. The total energy deposition also increases with the voltage [Fig. 1(b)].

Light generation efficiency has weak dependence on applied voltage [Fig. 1(c)]. Since these effects become more pronounced in some of the following results, we will discuss the factors that govern light generation efficiency here. As the gap voltage is increased beyond the breakdown voltage, avalanche takes place, and source functions for electron impact excitation reactions increase rapidly. During this phase, light generation efficiency increases with applied voltage. When the bulk plasma has achieved a quasisteady state density, it is analogous to the positive column of a direct-current (dc) discharge and so clamps to a small E/N that is necessary for maintaining current continuity. The remaining gap voltage appears across the cathode fall. As discussed in Paper I, the highest electron temperatures, and hence excitation effi-

ciency, occurs during the high E/N avalanche phase of operation. As the voltage increases, thereby requiring more current to charge the dielectric capacitance, the avalanche phase constitutes a smaller fraction of the total current pulse. The remainder of the longer current pulse consists of a less efficient low E/N positive column phase having lower electron temperature. The end result is that as the voltage increases, the PDP cell spends more time in the energy-inefficient discharge phase and so the light generation efficiency does not increase and, depending on conditions, may decrease [Fig. 1(c)]. The scaling depends on geometrical factors. For example, the effect is less pronounced at low applied voltage because the sheaths are thicker and Xe^* is produced, on the average, further from the top dielectric surface. As a result its effective lifetime in the cell is longer because of slower diffusion loss to walls allowing more time for conversion to Xe_2^* . This results in an improvement in light generation efficiency.

Up to a limit, the PDP light generation efficiency will increase if lower frequencies (longer interpulse times) are used. Although little power is dissipated beyond the 6 μs considered here, the lifetime of $\text{Xe}(6s)$ metastable is longer. It is desirable to allow sufficient interpulse time to elapse to allow the metastable to be fully converted to either the rapidly radiating Xe_2^* or the radiating resonant, but radiation trapped, multiplet partners.

The dimensions of the PDP cell are such that the breakdown voltage for a discharge between $E1$ and $E2$ is usually larger than that between the top electrodes and the bottom address electrode, which is grounded. This scaling can be attributed to a large proportion of the voltage between $E1$ and $E2$ being dropped through the intervening dielectric, compared to the voltage between either $E1$ or $E2$ and the address electrode. After the discharge has been quenched, there are two opposing electric fields in the plasma, one originating from the external supply and the other from the charge on the dielectric surfaces. The net affect of these opposing fields is to produce a small field across the plasma. When the external voltage is turned off, one of these opposing fields (due to external supply) is removed and the potential drop across the cell increases. If charging of the dielectric is sufficient, the potential drop between the top and bottom electrodes can be large enough to initiate a second, albeit less intense, discharge.

For example, the electron density is shown in Fig. 2(a) at 6 μs (just prior to turning off the voltage) and 6.1 μs (after turning off the voltage). A secondary discharge has taken place between $E2$ and the bottom address electrode, increasing the electron density and shifting its maximum towards the now positively biased address electrode. The intensity of visible light emission proportionately increases due to the secondary discharge [Fig. 2(b)]. To obtain this secondary discharge, the fall time of the trailing edge of the voltage pulse should be as short as possible. The additional fluence is obtained, however, at the expense of more power dissipation and partial neutralization of the charge on the dielectric surfaces, which increases the breakdown voltage for the next pulse. The aspect ratio of the cell and shape of the voltage pulse should be chosen so that one can make optimum use of

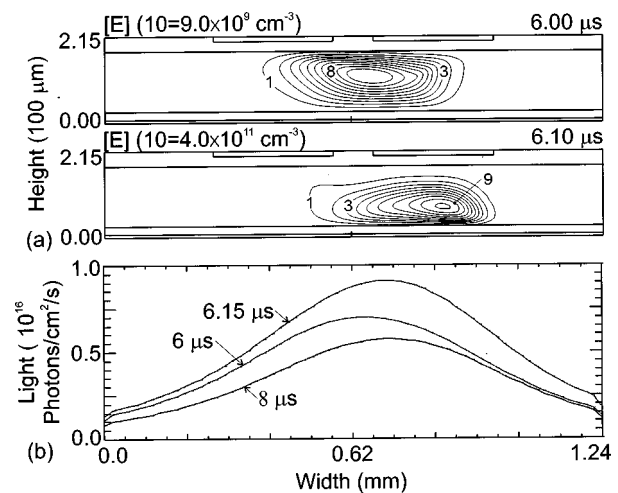


FIG. 2. PDP cell properties before and after the termination of the voltage pulse. (a) Electron density at 6 and 6.1 μs . (b) Visible photon flux at different times. Operating conditions are similar to the base case and $V_{E2} = 190 \text{ V}$ during the second pulse. Electron density plots have 11 contours, which are uniformly spaced between 0 and the specified maximum density.

the secondary discharge and still have reasonably low operating voltages for following pulses.

The consequences of gas pressure on the total visible light emission from the top of the cell during the second cycle (4–10 μs), total energy deposition, and light generation efficiency are shown in Fig. 3. Visible light is indirectly produced by the excited states of Xe (Xe^* and Xe^{**}) and the dimer Xe_2^* . As discussed in Paper I, Xe_2^* typically contributes more to visible light emission than Xe^* and Xe^{**} for our conditions since UV radiation from Xe_2^* is optically

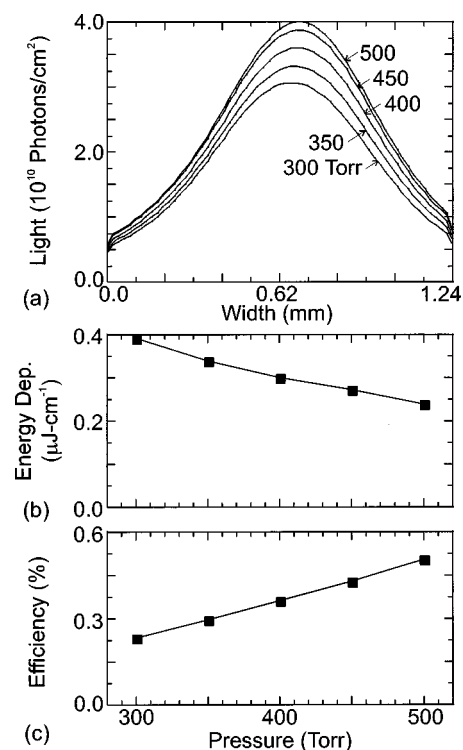


FIG. 3. Effect of gas pressure on cell properties (4–10 μs): (a) Visible light fluence, (b) total energy deposition, and (c) light generation efficiency.

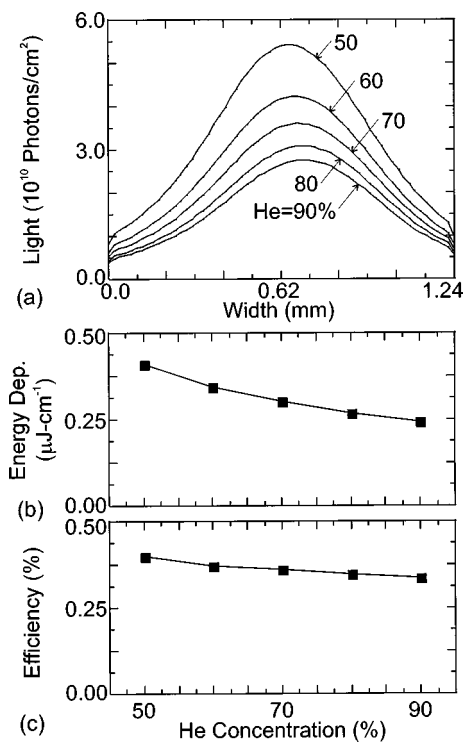


FIG. 4. Effect of He concentration on cell properties (4–10 μs): (a) Visible light fluence, (b) total energy deposition, and (c) light generation efficiency.

thin and the monomer excited states readily convert to Xe_2^* during and after the discharge through three-body collisions. Since Xe_2^* more efficiently contributes to visible light generation and more Xe_2^* are produced at higher pressures (because three body collisions are more efficient), the visible light fluence generally increases as the gas pressure is raised [Fig. 3(a)]. The values of pd (pressure times distance) in PDP cells are generally on the right side of the Paschen curve where breakdown voltage increases with pd .^{8,9} As a result, as the pressure is increased, the minimum voltage required to sustain the discharge increases. The gap voltage, therefore, falls below the sustaining voltage at earlier times with less charging of the dielectrics at higher pressures, which results in less energy dissipation [Fig. 3(b)]. More light output and less energy expenditure at higher pressures directly translates into higher efficiency [Fig. 3(c)]. In addition to the higher efficiency and larger light output, switching is also faster at high pressures because the source functions for electron-impact reactions (proportional to gas number density) are larger. It appears advantageous to operate PDP cells at as high a pressure as practical for a given voltage.

We also investigated the consequences of He/Ne concentrations on the PDP cell performance, while keeping the Xe concentration at 4%. The total visible light emission during the second cycle (4–10 μs), energy deposition and light generation efficiency are shown in Fig. 4 as a function of He concentration. He has a larger electron momentum transfer cross-section and collision frequency, ν_m at low and moderate energies than Ne.¹⁰ Since energy loss collisions are primarily with xenon, the increase in ν_m with more He for the same values of E/N produces a lower electron temperature. This scaling results in smaller rate coefficients for high

threshold electron impact processes. The minimum value of E/N required to sustain a discharge is therefore larger in He rich gas mixtures and, for the same applied voltage, less charging of the dielectrics is required before the discharge is extinguished. The end result is that less total excitation occurs during the shorter pulse, and so visible light fluence and energy deposition are lower [Figs. 4(a) and 4(b)] with increasing He.

If the only consequence of operating in He rich gas mixtures was to shorten the discharge pulse duration, the efficiency would have increased since the device spends less time in the energy-inefficient positive column phase. However, as shown in Fig. 4(c), the efficiency actually decreases with increasing He concentration. This scaling results from most of the two- and three-body collisions that directly or indirectly generate UV emitting Xe excited states having higher rate coefficients for collisions with Ne than He.⁴ Two-body collisions that involve excitation transfer or charge exchange are also more effective in Ne rich mixtures than He because Ne is more readily excited (or ionized) and therefore the Ne excited state (or ion) density is larger for a given E/N . These additional factors enable the light emission to increase at a faster rate than what would have been possible with only an increase of the length of the discharge, and as a result the device efficiency improves when Ne concentration is increased. It appears that optimizing gas composition is perhaps a more viable alternative for enhancing PDP cell luminosity compared to increasing the applied voltage.

In addition to operating conditions and gas composition, cell design (materials and dimensions) also has a strong influence on PDP characteristics. The consequences of spacing between $E1$ and $E2$ [l_e in Fig. 1(a) of Paper I] on total visible light emission during the 4–10 μs time period, total energy deposition, and light generation efficiency are shown in Fig. 5. As the electrodes are brought closer together, the proportion of applied voltage that drops across the intervening dielectric decreases and so the effective gap voltage increases. Since the dielectrics must now charge to a larger potential to reduce the gap voltage below the threshold for sustaining the discharge, the total fluence of current through the PDP cell increases, resulting in more production of excited state Xe and Xe_2^* and more visible light emission [Fig. 5(a)]. From a circuit viewpoint, moving the electrodes closer together increases their mutual capacitance, thereby requiring more current to charge. The energy deposition in the plasma also increases at smaller interelectrode spacing because of the larger total fluence of current through the device [Fig. 5(b)].

The consequences of decreasing l_e are similar to those for increasing the applied voltage amplitude because changing l_e dominantly affects only effective gap voltage. Light generation efficiency, therefore, exhibits the same weak dependence on electrode spacing as for applied voltage. To obtain the same luminosity and efficiency, one can decrease l_e while reducing the operating voltage amplitude. Smaller interelectrode distances will also minimize interaction between adjacent cells since light emission is more peaked towards the center, as shown in Fig. 5(a). If the interelectrode spacing is made very small ($l_e < 10 \mu\text{m}$), one may encroach

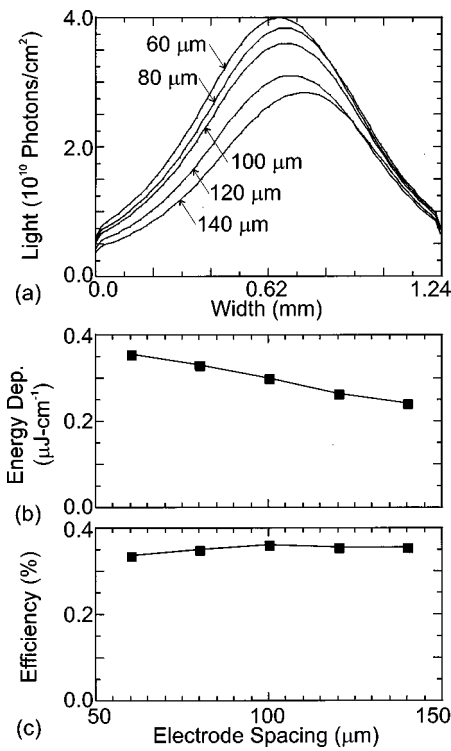


FIG. 5. Effect of electrode spacing on cell properties (4–10 μs): (a) Visible light fluence, (b) total energy deposition, and (c) light generation efficiency.

on the near side of the Paschen's curve, which will increase the breakdown voltage instead of decreasing it.

As shown in Figs. 6 and 7 for the 4–10 μs period, decreasing the dielectric thickness (d_d) or increasing the rela-

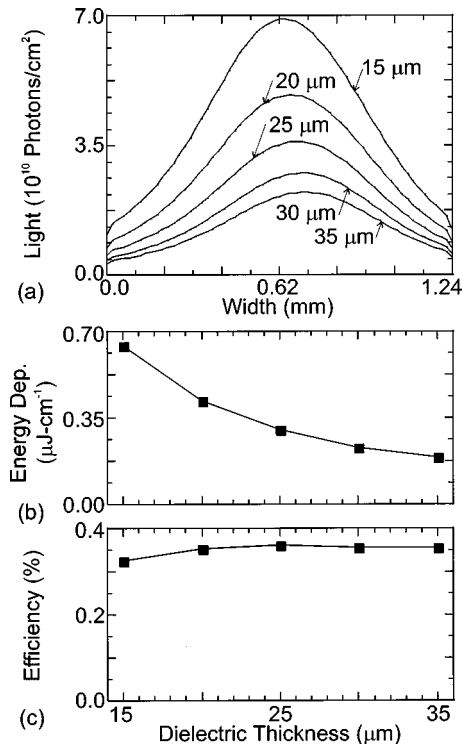


FIG. 6. Effect of dielectric thickness on cell properties (4–10 μs): (a) Visible light fluence, (b) total energy deposition, and (c) light generation efficiency.

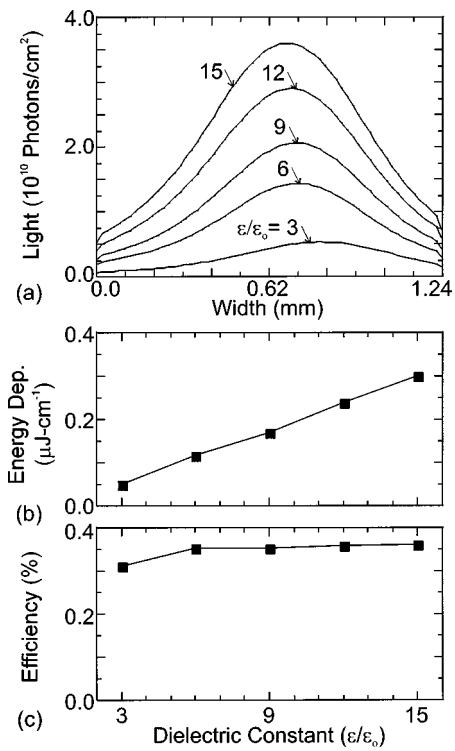


FIG. 7. Effect of relative permittivity of the upper dielectric on cell properties (4–10 μs): (a) Visible light fluence, (b) total energy deposition, and (c) light generation efficiency.

tive permittivity of the upper dielectric (ϵ) have a similar effect on light emission, total energy deposition, and light generation efficiency as decreasing the electrode spacing. As ϵ is increased or d_d is decreased, the penetration of the interelectrode electric field into the gap and the effective gap voltage increases, which is purely a geometrical effect. From a circuit viewpoint, decreasing d_d or increasing ϵ increases the capacitance of the electrode dielectric stack. With the larger voltage across the gap, and larger capacitance of the dielectric, more current is required to charge the dielectrics to reduce the gap voltage below the threshold for sustaining the discharge. More energy is deposited in the plasma [Figs. 6(b) and 7(b)] and the corresponding visible light fluence is larger [Figs. 6(a) and 7(a)]. The influence of ϵ or d_d on light generation efficiency is similar in nature to that of the applied voltage. As ϵ is decreased or d_d is increased from the base case conditions ($\epsilon/\epsilon_0 = 15$, $d_d = 25 \mu\text{m}$, $V_0 = 180 \text{V}$), the effective gap voltage decreases, the discharge becomes less intense, and light generation efficiency decreases. As d_d is decreased below 25 μm , the effective gap voltage increases, the cell spends more time in the energy-inefficient discharge phase, and light generation efficiency decreases.

The effects of electrode length [l in Fig. 1(a) of Paper I] on the total visible light emission during the 4–10 μs time period, total energy deposition, and light generation efficiency are shown in Fig. 8. As we discussed in Paper I, the gas initially breaks down close to the adjacent edges of $E1$ and $E2$ where the electric field is the largest. As the voltage drop in that region decreases due to dielectric surface charging, the discharge moves towards the outer edges of the electrodes, a process which reduces the electric field in the gap

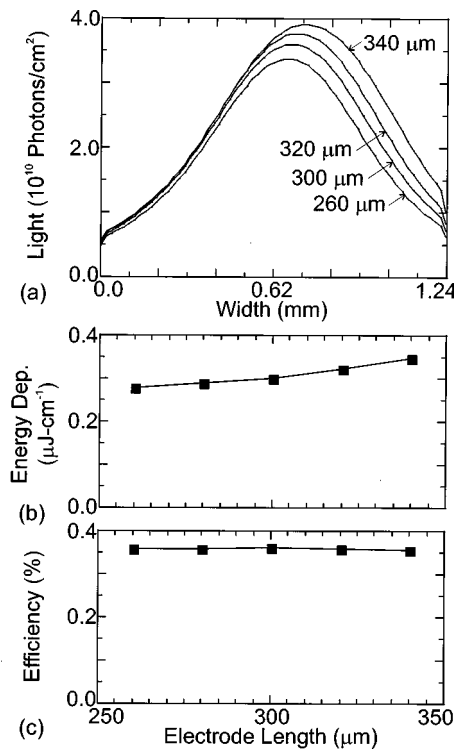


FIG. 8. Effect of electrode length on cell properties (4–10 μs): (a) Visible light fluence, (b) total energy deposition, and (c) light generation efficiency.

due to the effective lengthening of the interelectrode distance. The discharge is extinguished when either the whole surface under the electrodes is charged or the electric field falls below the self-sustaining value, whichever comes first. For the range of electrode lengths investigated, the discharge is quenched when the plasma expands to reach the end of $E2$. Since the discharge is maintained for a longer period of time when the electrodes are larger and more surface charging has to take place, more visible light emission is produced [Fig. 8(a)]. Note that the light fluence increases more towards the right side of the cell where $E2$ is located, and is broader due to the larger electrode size. As the electrode area increases, total energy deposition increases because of larger current fluence [Fig. 8(b)] required to charge the larger capacitance. However, for the range of electrode lengths that we investigated, electrode length does not have a significant effect on light generation efficiency.

The consequences of the interdielectric spacing (d) on total visible light emission during the second pulse (4–10 μs), total energy deposition, and light generation efficiency are shown in Fig. 9. Visible light fluence has a nonmonotonic dependence on d . When the gap is small ($d=100 \mu\text{m}$), the equipotential planes are more horizontal between the top and bottom electrodes at the beginning of the pulse than at larger values of d due to closer proximity of the potential of the bottom charged dielectric. Ions generated below $E2$ therefore are dominantly collected on the bottom dielectric surface during the second pulse and the discharge mainly takes place between $E2$ and the grounded address electrode. The discharge and visible light emission are, however, weak because the positive charge left on the lower dielectric surface from the first pulse reduces the gap voltage

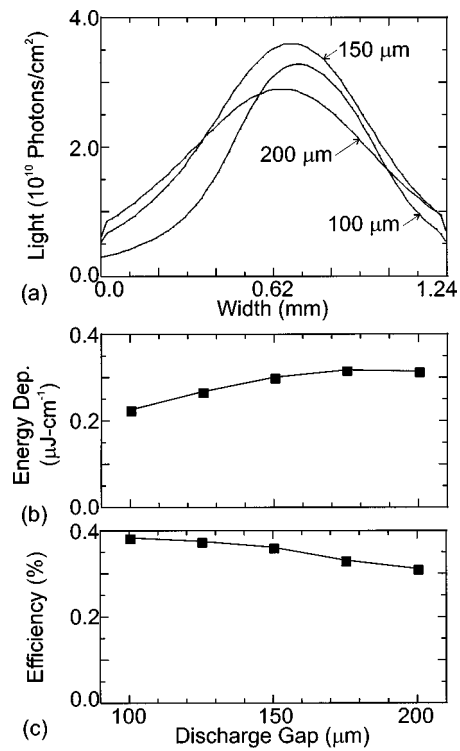


FIG. 9. Effect of dielectric spacing on cell properties (4–10 μs): (a) Visible light fluence, (b) total energy deposition, and (c) light generation efficiency.

considerably. The discharge characteristics at this interdielectric spacing may evolve during subsequent pulses but the interference from the bottom address electrode is expected to disrupt the normal PDP operation. As d is increased, the device transitions to the normal PDP behavior and the light intensity increases because the discharge between $E1$ and $E2$ is sustained for a longer period of time [Fig. 9(a)]. Once the PDP cell is operating normally, the grounded address electrode does not significantly effect the electrodynamics of the PDP cell during the discharge, and the upper dielectric surface charge and power deposition [Fig. 9(b)] do not change significantly.

Excited states of the Xe are dominantly produced near the upper electrode. Increasing the interdielectric spacing means that Xe^* and Xe^{**} are produced further from the phosphor, and are quenched to a greater degree before they are within a few absorption wavelengths of the phosphor. This is illustrated in Fig. 10 by comparing Xe^* densities and light intensity at 4.5 μs for $d=150$ and 200 μm . Although the peak Xe^* density below the top dielectric is actually higher for $d=200 \mu\text{m}$ [Fig. 10(a)], the density is significantly lower level near the bottom dielectric where the phosphor is located [Fig. 10(b)]. As a result the visible light emission decreases [Fig. 10(c)]. Since power deposition changes little with d during normal PDP operation, the light generation efficiency decreases due to less optimum excited state distribution and subsequent radiation transport. The interdielectric spacing appears to be a critical factor in PDP cell design, with an optimum value being sufficiently large to eliminate interference and minimize ion sputtering of the phosphor, but sufficiently small to optimize excited state and radiation transport.

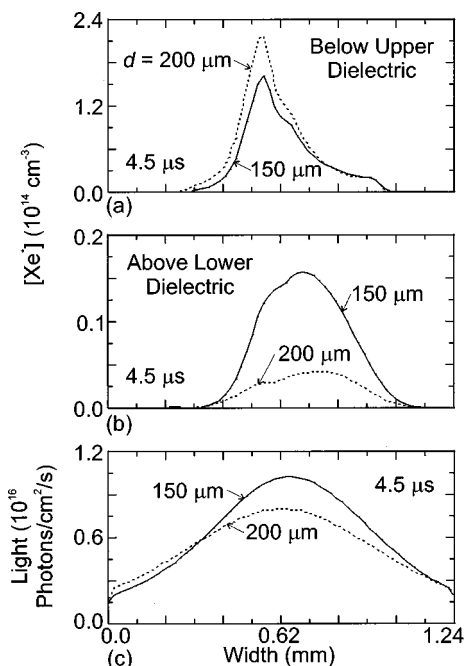


FIG. 10. Cell properties for dielectric spacings of 150 and 200 μm : (a) Xe^* density 10 μm below the top dielectric, (b) Xe^* density 10 μm above the bottom dielectric, and (c) visible photon flux at 4.5 μs .

IV. CONCLUDING REMARKS

The operation of a coplanar-electrode PDP cell sustained in He/Ne/Xe gas mixtures has been discussed for a variety of operating conditions and cell dimensions. For the conditions examined UV radiation from Xe_2^* was found to contribute more to visible light emission than the excited states of Xe because the radiation from Xe_2^* is optically thin and the excited Xe atoms readily convert to Xe_2^* after the discharge pulse through three-body collisions. Increasing the gas pressure shifted the reaction mechanism towards the production of more Xe_2^* , which led to the production of more visible light. For constant voltage, power deposition during the low efficiency positive column phase decreased with increasing pressure because the minimum sustaining electric field increases and the discharge is extinguished more quickly. Increased visible light production and decreased power deposition at higher pressures results in higher efficiency. Gas mixtures with larger Ne concentrations generated more visible light because the discharge was sustained for a longer period of time. Light generation efficiency was also higher in Ne rich gas mixtures because Xe_2^* is produced more efficiently due to three-body collisions with Ne than with He.

The optimum voltage (highest efficiency) is bound on the low side by potentials for which excited states of Xe are

not produced efficiently. When the gap voltage exceeds the optimum, more time is spent in the energy inefficient positive column phase, thus decreasing the overall light generation efficiency. The same trends were observed when any of the factors that influence gap voltage were changed including applied voltage amplitude, dielectric thickness, dielectric permittivity, and interelectrode spacing. For the PDP dimensions we considered, a secondary discharge between the electrodes and the grounded address electrode occurred when the voltage pulse was turned off thereby increasing visible light emission. Light production was, however, at the expense of partial neutralization of charge on the dielectric surfaces.

Although considerable improvements can be made in PDP efficiency by optimizing the operating conditions and cell dimensions, it appears that selection of gas mixtures that favor the production of more Xe_2^* molecules can lead to significant improvements in light generation efficiency. The main mechanism through which Xe_2^* is quenched is radiative decay due to its short lifetime so UV production is very efficient. On the other hand, there are many mechanisms that compete directly with radiative decay for Xe^* and Xe^{**} (superelastic relaxation, radiation trapping, multistep ionization) so UV production efficiency is lower. UV radiation from Xe^* and Xe^{**} is also optically thick so photons from only a small region are effectively useful for visible light generation.

ACKNOWLEDGMENTS

This work was supported by LG Electronics Inc. and the National Science Foundation (ECS 94-04133, CTS 94-12565). The authors thank K. J. Shin and R. Veerasingam for insight into PDP operation.

- ¹A. Sobel, IEEE Trans. Plasma Sci. **19**, 1032 (1991). A. Sobel, Sci. Am. **278**, 70 (1998).
- ²*Electronic Display Devices*, edited by S. Matsumoto (Wiley, New York, 1990), p. 131.
- ³J. A. Castelano, *Handbook of Display Technology* (Academic, New York, 1992), p. 111.
- ⁴S. Rauf and M. J. Kushner, J. Appl. Phys. **85**, 3460 (1999).
- ⁵C. Punset, J. P. Boeuf, and L. C. Pitchford, J. Appl. Phys. **83**, 1884 (1998).
- ⁶S. Sato, H. Yamamoto, Y. Shirochi, I. Iemori, N. Nakayama, and I. Morita, IEEE Trans. Electron Devices **23**, 328 (1976).
- ⁷D. Braun, V. Gibalov, and G. Pietsch, Plasma Sources Sci. Technol. **1**, 166 (1992).
- ⁸M. A. Lieberman and A. J. Lichtenberg, *Principles of Plasma Discharges and Materials Processing* (Wiley, New York, 1994), p. 460.
- ⁹B. M. Smirnov, *Physics of Weakly Ionized Gases* (Mir, Moscow, 1981), p. 367.
- ¹⁰M. Hayashi, Report IPPJ-AM-19 (Nagoya University, 1981).